Schizophrenia Bulletin vol. 43 no. 3 pp. 620–632, 2017
doi:10.1093/schbul/sbw109
Advance Access publication August 18, 2016

Abnormal Grey Matter Arteriolar Cerebral Blood Volume in Schizophrenia Measured With 3D Inflow-Based Vascular-Space-Occupancy MRI at 7T

Jun Hua*[,1,2], Allison S. Brandt[3], SeungWook Lee[4], Nicholas I. S. Blair[4], Yuankui Wu[1,2,5], Su Lui[6,7], Jaymin Patel[4], Andreia V. Faria[1], Issel Anne L. Lim[1,2], Paul G. Unschuld[8], James J. Pekar[1,2], Peter C. M. van Zijl[1,2], Christopher A. Ross[3,9,10], and Russell L. Margolis[3,9]

[1]The Russell H. Morgan Department of Radiology and Radiological Science, Division of MR Research, Johns Hopkins University School of Medicine, Baltimore, MD; [2]F.M. Kirby Research Center for Functional Brain Imaging, Kennedy Krieger Institute, Baltimore, MD; [3]Department of Psychiatry and Behavioral Sciences, Johns Hopkins University School of Medicine, Baltimore, MD; [4]Department of Biomedical Engineering, Johns Hopkins University, Baltimore, MD; [5]Department of Medical Imaging, Nanfang Hospital, Southern Medical University, Guangzhou, China; [6]Department of Radiology, Huaxi MR Research Center (HMRRC), West China Hospital of Sichuan University, Chengdu, China; [7]Department of Radiology, the Second Affiliated Hospital, Wenzhou Medical University, Wenzhou, China; [8]Division of Psychiatry Research and Psychogeriatric Medicine, University of Zurich, Zurich, Switzerland; [9]Department of Neurology and Program in Cellular and Molecular Medicine, Johns Hopkins University School of Medicine, Baltimore, MD; [10]Departments of Neuroscience and Pharmacology, Johns Hopkins University School of Medicine, Baltimore, MD

*To whom correspondence should be addressed; Department of Radiology, Johns Hopkins University School of Medicine, 707 N Broadway, Baltimore, MD 21205, US; tel: 443-923-3848, fax: 443-923-9505, e-mail: jhua@mri.jhu.edu

Metabolic dysfunction and microvascular abnormality may contribute to the pathogenesis of schizophrenia. Most previous studies of cerebral perfusion in schizophrenia measured total cerebral blood volume (CBV) and cerebral blood flow (CBF) in the brain, which reflect the ensemble signal from the arteriolar, capillary, and venular compartments of the microvasculature. As the arterioles are the most actively regulated blood vessels among these compartments, they may be the most sensitive component of the microvasculature to metabolic disturbances. In this study, we adopted the inflow-based vascular-space-occupancy (iVASO) MRI approach to investigate alterations in the volume of small arterial (pial) and arteriolar vessels (arteriolar cerebral blood volume [CBVa]) in the brain of schizophrenia patients. The iVASO approach was extended to 3-dimensional (3D) whole brain coverage, and CBVa was measured in the brains of 12 schizophrenia patients and 12 matched controls at ultra-high magnetic field (7T). Significant reduction in grey matter (GM) CBVa was found in multiple areas across the whole brain in patients (relative changes of 14%–51% and effect sizes of 0.7–2.3). GM CBVa values in several regions in the temporal cortex showed significant negative correlations with disease duration in patients. GM CBVa increase was also found in a few brain regions. Our results imply that microvascular abnormality may play a role in schizophrenia, and suggest GM CBVa as a potential marker for the disease. Further investigation is needed to elucidate whether such effects are due to primary vascular impairment or secondary to other causes, such as metabolic dysfunction.

Key words: imaging/biomarker/vascular/perfusion/high field/psychosis

Introduction

Schizophrenia is a psychiatric disorder that is characterized by positive symptoms (eg, hallucinations, delusions, thought disorder), negative symptoms (eg, affective blunting, anhedonia), cognitive deficits, and social impairments.[1] While the acute phase of schizophrenia is predominantly defined by positive symptoms, long-term disability particularly relates to cognitive dysfunction.[2] Metabolic dysfunction in the brain may occur early and act causally in the disease pathogenesis.[3–5] As the supply of adequate oxygen and energy substrates for local metabolic demands is controlled by blood vessels in the brain, microvascular abnormalities may contribute to the neuropathology of the disease.[6] Moreover, cerebrovascular pathology is frequently associated with cognitive dysfunction in general.[7] Cerebral blood volume (CBV) is a sensitive physiological parameter that reflects the homeostasis of the microvasculature. It has been demonstrated that baseline CBV measures correlate with basal metabolism[8,9] and can predict progression to psychosis.[5,10] In addition, baseline CBV is a major modulator for the blood-oxygen-level-dependent (BOLD) effect,[11–13] which has been used in numerous functional MRI (fMRI) studies in schizophrenia. Since BOLD fMRI measures relative changes between the baseline and activated states

(for instance, during a functional task), the investigation of potential alterations in baseline hemodynamic parameters in patients may provide crucial information for proper interpretation of BOLD signal changes detected in fMRI studies of schizophrenia.

Abnormalities in total CBV (a measure that includes blood within arterial, capillary and venous vessels) in schizophrenia have been studied using contrast enhanced MRI methods, typically by acquiring images after intravenous injection of an exogenous contrast agent. Widespread reductions in total CBV in schizophrenia patients compared to controls have been observed in both hemispheres of the brain,[14] frontal cortex,[10,15,16] and visual cortex.[15] There is some evidence of a negative correlation between disease duration and total CBV in the frontal lobe.[17] Increase in total CBV in schizophrenia, found less frequently than decreased total CBV, has been reported in the cerebellum,[18,19] basal ganglia and some regions in the occipital lobe,[19] orbitofrontal cortex,[10] and hippocampus.[5,10,20,21] In addition, altered cerebral blood flow (CBF) in schizophrenia has been detected with various methods such as MRI, positron emission tomography (PET) and single-photon emission computerized tomography (SPECT),[14–16,22–35] although results thus far have been conflicting and inconclusive.

Histological studies in postmortem human brain tissue have not revealed significant differences between schizophrenia patients and controls in capillary diameter, length, cross-sectional area and length density in several cortical and sub-cortical regions.[36–38] This implies that the total CBV changes measured in previous studies may come from microvascular compartments other than the capillaries, ie, arterial, arteriolar or venous vessels. Blood vessels in the brain are predominantly regulated by vascular smooth muscle cells in the arterioles and pial arteries and, to a lesser extent by the pericytes in the capillaries.[39–47] Small arteries and arterioles are most responsive to changes in metabolism.[41–45] Therefore, the measurement of changes in arteriolar blood vessels separately may furnish information that is not obtainable from total CBV and CBF measures, and may provide a more sensitive quantitative marker for the disease. Based on the widespread decrease of total CBV and unchanged capillary measures reported in the literature, we hypothesized that CBV of pial arteries and arterioles (arteriolar cerebral blood volume [CBVa]) may be significantly reduced in some cortical and sub-cortical regions in schizophrenia.

To test this hypothesis, we applied the recently developed inflow-based vascular-space-occupancy (iVASO) MRI technique[48–55] with large-vessel signal crushing to investigate potential abnormalities in CBVa in the grey matter (GM) of the brain in schizophrenia patients compared with matched control subjects. The iVASO approach is completely noninvasive, and does not require the administration of exogenous contrast agents. We have extended iVASO MRI from a single-slice technique to a 3-dimensional (3D) sequence with whole brain coverage. This study was performed on ultra-high magnetic field (7.0 Tesla or 7T) to take advantage of the enhanced sensitivity. Part of this work has been reported in abstract form.[56]

Methods

Participants

Twelve patients with a diagnosis of schizophrenia or schizoaffective (n = 2) disorder and 12 age and sex matched normal controls were recruited and scanned in this Johns Hopkins Institutional Review Board approved study. All participants gave written informed consent before scanning. Demographic data and clinical measures are summarized in table 1. None of the subjects had other neurologic history or neurological signs on exam, or a history of vascular diseases. As tobacco smoking could potentially affect brain perfusion, current smoking status (cigarettes smoked per day) was determined for patients and controls. Current schizophrenia symptom severity was assessed with the Brief Psychiatric Rating Scale (BPRS).[57] Diagnosis was based on clinical records and clinical referrals at the point of ascertainment, and was confirmed by symptom evaluation on entry into the study. All patients, but none of the controls, were receiving antipsychotic medicines. A Montreal Cognitive Assessment (MoCA)[58] was performed on each participant on the day of scanning.

MRI

All scans were performed on a 7T Philips MRI scanner (Philips Healthcare). A 32-channel phased-array head

Table 1. Demographic and Clinical Data for the Study Participants

	Control Subjects	Schizophrenia Patients	*P* Value[a]
N	12	12	N/A
Sex (male)	75%	75%	1
Age (y)	37.4 ± 16.6[b]	39.6 ± 18.4	.73
Disease duration (y)	N/A	19.0 ± 17.8	N/A
Smoking status (cig/d)	1.7 ± 3.1	2.3 ± 2.4	.55
BPRS score[c]	23.1 ± 3.4	38.1 ± 8.4	<.00001
Medication[d]	N/A	93.9 ± 130.7	N/A
MoCA[e] score	25.5 ± 3.0	22.8 ± 3.8	.04

Note: [a]*P* values from 2-sample *t* tests between the 2 groups for age, smoking status, Brief Psychiatric Rating Scale (BPRS) and Montreal Cognitive Assessment (MoCA) scores; or from chi-square test for the categorical variable sex.
[b]Mean ± SD.
[c]Please see Methods section for references. BPRS subscales are reported in supplementary table 1.
[d]Medication reported with derived chlorpromazine equivalent dose in dose-year (milligram).
[e]Please see Methods section for references. MoCA subscales are reported in supplementary table 2.

coil (Nova Medical) was used for RF reception and a head-only quadrature coil for transmit. High-resolution anatomical images were acquired with a 3D magnetization prepared 2 rapid acquisition gradient echoes (MP2RAGE) sequence[59,60] (voxel = 0.65 mm isotropic) to minimize B1 field inhomogeneity induced artifacts at 7T.

GM CBVa was measured using 3D iVASO MRI with whole brain coverage. In iVASO MRI, a spatially selective inversion is employed to zero out (null) the inflowing arterial blood signal. CBVa can then be calculated from the difference signal between the arterial blood nulled scan and a control scan without blood nulling.[48,50] Interleaved nulling and control images are acquired at multiple post-inversion delay times (TI) to account for the heterogeneity of vascular transit times, from which absolute CBVa can be quantified using the iVASO theory.[48] To sensitize this method to CBVa predominantly in the pial arteries and arterioles, crushing gradients can be incorporated to suppress signals from fast-flowing blood in large arteries. The iVASO approach was originally developed in single-slice mode using a gradient-echo (GRE) echo-planar-imaging (EPI) readout. We have now extended it to a 3D sequence with whole brain coverage by adopting a 3D spoiled fast GRE (also known as T1-enhanced turbo field echo, TFE or TurboFLASH) readout. This readout has been preciously implemented for VASO MRI at 7T, which showed less geometrical distortion than EPI and low power deposition.[61] A low–high (also known as "centric") phase encoding was used so that the center of k-space, which determines the gross signal intensity in the image, was acquired at the first echo. A hyperbolic secant adiabatic pulse optimized in our previous 7T work on the same scanner was used for spatially nonselective inversion.[61] An optimized frequency offset corrected inversion (FOCI) pulse was used for spatially selective inversion in iVASO to ensure sharp edges of the inversion slab. The following iVASO parameters were used: TR/TI = 10 000/1383, 5000/1093, 3800/884, 3100/714, 2500/533, and 2000/356 ms; 3D fast GRE readout (TI calculated based on a blood T1 value of 2587 ms at 7T[62]), TR_{GRE} (this is the time of repetition [TR] between 2 echoes during the fast GRE readout)/TE_{GRE} = 4.2/2.2 ms; voxel = $3.5 \times 3.5 \times 5\,mm^3$, 20 slices; parallel imaging acceleration (SENSE) = 2 × 2; crusher gradients of $b = 0.3\,s/mm^2$ and velocity encoding (Venc) = 10 cm/s on z-direction. A reference scan (TR = 20 s, other parameters identical) was obtained to determine the scaling factor M0 in iVASO images so that absolute CBVa values can be calculated.

Data Analysis

The statistical parametric mapping (SPM) software package (Version 8, Wellcome Trust Centre for Neuroimaging; http://www.fil.ion.ucl.ac.uk/spm/) and other in-house code programmed in Matlab (MathWorks) were used for image analysis. iVASO images were motion corrected using the realignment routine in SPM. Anatomical images were co-registered with iVASO images and normalized to the Montreal Neurological Institute (MNI) space using SPM. GM, white matter (WM), and cerebrospinal fluid (CSF) maps were generated from the anatomical images using the SPM segmentation algorithm. No spatial smoothing was performed in the analysis. The surround subtraction method[63] was used to calculate the difference signal from the nulling and control iVASO images. Partial volume effects of WM and CSF on the iVASO difference signal in GM were corrected.[64] A signal-to-noise ratio (SNR) threshold of 1 SD below the mean SNR was used to exclude voxels with insufficient SNR from further analysis.[48] Whole-brain GM CBVa maps were numerically fitted from the iVASO difference signals at all TIs with the iVASO equations.[48] Two-sample t tests were performed to examine group difference in GM CBVa values in the whole brain on a voxel-by-voxel basis. Age, sex, smoking status, regional GM volume from anatomical scans and residual motion parameters (after motion correction) were all accounted for as covariates in the analysis. Significant clusters of decreased or increased GM CBVa were identified, and clusters of 10 or fewer voxels were excluded. The IBASPM116 atlas[65–69] (PickAtlas software, Wake Forest University) was used to identify anatomical regions within the significant clusters (note that an anatomical region from the atlas may have both decreased or increased CBVa clusters in its sub-regions). Effect size was estimated with Cohen's d. Correlations between CBVa values and disease duration, antipsychotic medication dosage, BPRS and MoCA scores (including the total score and subscales for both BPRS and MoCA) were evaluated using adjusted R^2 from linear regression. Note that for correlations between CBVa and disease duration, BPRS and MoCA scores, partial correlations were calculated with age, smoking status, and medication dosage as covariates. Multiple comparisons were corrected with the false-discovery rate (adjusted $P < .05$).[70]

Results

As shown in table 1, age and sex were matched between schizophrenia patients and control subjects ($P > .1$). The average numbers of cigarettes smoked per day were comparable between the 2 groups. Schizophrenia patients had significantly higher BPRS scores ($P < .001$), and slightly lower total MoCA scores ($P < .05$) compared to control subjects. No significant differences were found in motion parameters derived from the SPM realignment routine between the 2 groups. Figure 1a demonstrated a representative whole brain CBVa map calculated from the iVASO images from 1 subject.

Tables 2 and 3 summarize the main findings in the group comparisons. Widespread reduction of GM CBVa was found in multiple brain regions in schizophrenia

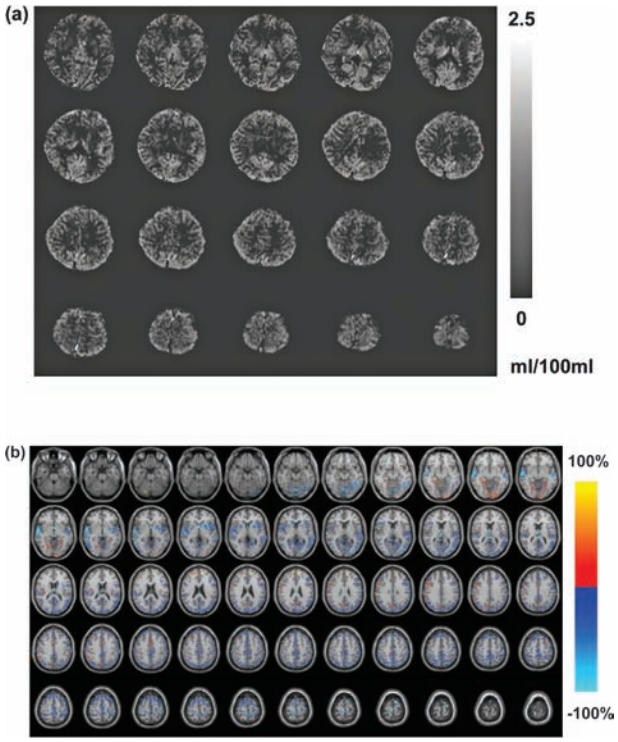

Fig. 1. (a) Representative whole brain arteriolar cerebral blood volume (CBVa) map (ml blood/100 ml brain tissue) calculated from the inflow-based vascular-space-occupancy (iVASO) images from 1 subject. (b) Map of relative CBVa changes between schizophrenia patients and control subjects overlaid on Montreal Neurological Institute (MNI) normalized anatomical images. The relative change is defined as [100 × (schizophrenia − control)/control] %. Only voxels that show significant CBVa difference between the 2 groups (adjusted $P < .05$) are highlighted.

patients compared to controls ($n = 12$) with relative changes of 14%–51% and effect sizes of 0.7–2.3. Most of these changes were detected in both hemispheres in corresponding regions, although the cluster sizes varied between the left and right hemispheres in some regions. There were also some GM CBVa increases detected in a few brain regions with relative changes of 16%–85% and effect sizes of 0.6–1.5. Some brain regions showed both decreased and increased GM CBVa values in different sub-regions. No significant difference was found in mean GM CBVa over the whole brain (including all GM voxels, not just significant clusters) between patients and controls. Figure 1b displays the regions with significant decreased or increased GM CBVa in schizophrenia patients on MNI normalized anatomical images, with an intensity reflecting the relative changes in each significant voxel.

We found significant negative correlations (figure 2) between disease duration and GM CBVa values in the superior temporal gyrus, middle temporal gyrus and Heschl's gyrus (also known as transverse temporal gyrus). Age, smoking status and medication dosage were included as covariates in the correlation analysis. The disease durations of the 12 patients included in this analysis can be split into 2 sub-groups with moderate ($n = 7$) or long ($n = 5$) disease duration, however the sample size of each sub-group was too small to detect significant differences between them. GM CBVa did not significantly correlate with BPRS and MoCA scores (including subscales for both BPRS and MoCA), and antipsychotic medication dosage in schizophrenia patients.

Discussion

The present study, to our knowledge, is the first to investigate microvascular alterations in arteriolar vessels in the brain of schizophrenia patients. Most previous studies in the literature measured total CBV and CBF in the brain (see Introduction), which reflects the sum of signals from the arterial, capillary and venous compartments in the microvasculature. However, different types of blood vessels have distinct functions and underlying physiology, and can be affected differentially by the pathology. A few studies have examined capillaries in postmortem human brain tissue from schizophrenia patients using microscopy,[36–38] but did not find significant changes when compared to normal brains. The arterioles are the most actively regulated blood vessels in the microvasculature, and thus may be more sensitive to metabolic disturbances or other functional alterations in the brain.[41–45] We therefore adopted the recently developed iVASO MRI approach to compare absolute CBV in pial arteries and arterioles (CBVa) in the brains of schizophrenia patients and control subjects. To achieve whole brain coverage, we extended iVASO MRI from its original single slice version to a 3D pulse sequence using a 3D fast GRE readout. As a noninvasive MRI technique, iVASO MRI utilizes magnetically labeled proton spins in the water molecules in blood as intrinsic endogenous contrast agents to measure absolute CBVa in physiological units (ml blood/100 ml brain tissue). This may be a potential advantage for clinical applications compared to the currently widely used total CBV methods that require the injection of exogenous contrast agents. Besides the invasiveness and inconvenience of contrast media injection, Gadolinium based contrast agents (the most common type) have been associated with nephrogenic systemic fibrosis in subjects with renal diseases.[71,72] More recently, concerns have been raised on brain deposits of such contrast agents long after the administration in subjects with normal renal function.[73]

The main finding from this study was the widespread reduction in CBVa in GM in schizophrenia patients compared to control subjects. This is congruent with previous reports of hypoperfusion in the brain of schizophrenia patients. Decrease in total CBV (sum of arterial, capillary and venous CBV) in schizophrenia has been observed[14] in the frontal[10,15,16] and occipital cortex.[15] Reduced CBF was also found in the frontal lobe,[16,22–34] temporal lobe,[22,27–29,32,34] parietal lobe,[22,23,26,29] occipital lobe,[15,25,30]

Table 2. Reduced GM CBVa in Schizophrenia Patients Compared to Controls in Various Brain Regions

Region[a]	Hemisphere	Cluster Size[b]	Cluster Peak[c] (mm, MNI)			CBVa (ml Blood/100 ml Tissue)				Relative Change (%)[d]	Effect Size[e]	Adjusted *P* Value
						Schizophrenia		Control				
			x	y	z	Mean	SD	Mean	SD			
Angular	L	333	−42	−70	44	0.76	0.24	1.21	0.29	−36.9	−1.75	.003
Angular	R	339	48	−64	38	0.84	0.16	1.15	0.16	−26.5	−1.97	.001
Calcarine	L	438	−16	−58	8	0.98	0.03	1.33	0.44	−26.3	−1.17	.044
Calcarine	R	242	10	−90	12	0.98	0.06	1.39	0.67	−29.3	−0.88	.05
Cingulum_Ant	L	47	0	20	26	1.06	0.09	1.48	0.42	−28.5	−1.42	.018
Cingulum_Ant	R	16	2	20	26	1.28	0.43	1.89	0.71	−32.0	−1.07	.049
Cingulum_Mid	L	306	0	−28	46	0.91	0.14	1.09	0.14	−16.6	−1.31	.02
Cingulum_Mid	R	260	2	−12	30	0.89	0.15	1.08	0.10	−16.9	−1.50	.013
Cingulum_Post	L	41	−2	−40	16	0.91	0.16	1.12	0.27	−19.1	−1.00	.05
Cingulum_Post	R	62	6	−44	18	0.87	0.17	1.20	0.43	−28.0	−1.07	.05
Cuneus	L	383	−8	−70	26	0.82	0.15	1.11	0.20	−26.9	−1.78	.003
Cuneus	R	258	14	−78	42	0.77	0.21	1.14	0.30	−32.6	−1.49	.01
Frontal_Inf_Oper	L	162	−56	8	22	1.12	0.20	1.58	0.63	−29.0	−1.01	.05
Frontal_Inf_Oper	R	94	54	14	38	1.20	0.78	1.84	0.54	−35.1	−1.00	.05
Frontal_Inf_Tri	L	229	−44	24	2	1.07	0.15	1.53	0.63	−30.2	−1.05	.05
Frontal_Inf_Tri	R	75	56	34	16	1.23	0.75	1.83	0.94	−32.9	−0.74	.05
Frontal_Mid	L	384	−44	14	52	0.84	0.24	1.14	0.22	−26.4	−1.36	.017
Frontal_Mid	R	293	32	34	48	0.86	0.20	1.17	0.27	−26.8	−1.39	.015
Frontal_Sup	L	391	−16	40	46	0.86	0.25	1.46	0.35	−41.4	−2.05	.001
Frontal_Sup	R	487	24	26	58	0.83	0.25	1.28	0.32	−34.8	−1.59	.006
Frontal_Sup_Medial	L	227	−8	34	58	0.99	0.25	1.46	0.42	−32.2	−1.42	.013
Frontal_Sup_Medial	R	216	6	40	42	1.00	0.38	1.78	0.86	−43.6	−1.21	.032
Heschl	L	68	−62	−12	8	1.14	0.24	1.58	0.55	−27.5	−1.07	.05
Heschl	R	13	44	−24	14	1.12	0.19	1.43	0.36	−21.7	−1.12	.043
Insula	L	211	−36	2	−4	1.20	0.44	1.92	0.94	−37.4	−1.02	.037
Insula	R	90	38	−28	20	1.36	0.64	1.96	0.63	−30.5	−0.98	.031
Lingual	L	244	−10	−56	2	1.03	0.09	1.68	0.81	−38.3	−1.16	.044
Lingual	R	170	16	−54	0	1.08	0.13	1.53	0.46	−29.3	−1.37	.02
Occipital_Inf	L	50	−36	−80	−12	1.26	0.63	1.98	0.96	−36.4	−0.92	.05
Occipital_Inf	R	80	48	−80	−2	0.97	0.18	1.47	0.74	−34.1	−0.97	.05
Occipital_Mid	L	782	−34	−82	32	0.86	0.15	1.47	0.88	−41.2	−1.00	.05
Occipital_Mid	R	386	28	−90	14	0.89	0.11	1.24	0.47	−28.4	−1.08	.05
Occipital_Sup	L	405	−18	−80	44	0.82	0.16	1.18	0.33	−30.5	−1.43	.014
Occipital_Sup	R	277	24	−80	42	0.87	0.11	1.14	0.26	−23.8	−1.40	.016
Paracentral_Lobule	L	233	−8	−38	70	0.80	0.28	1.45	0.99	−44.8	−0.93	.05
Paracentral_Lobule	R	179	4	−44	68	0.73	0.27	1.50	0.94	−51.3	−1.15	.043
Parietal_Inf	L	408	−44	−58	54	0.75	0.27	1.15	0.29	−34.5	−1.48	.01
Parietal_Inf	R	170	42	−54	52	0.82	0.22	1.12	0.22	−26.4	−1.38	.015
Parietal_Sup	L	351	−38	−66	52	0.67	0.29	1.18	0.30	−43.3	−1.80	.003
Parietal_Sup	R	352	28	−64	56	0.69	0.29	1.11	0.24	−37.7	−1.62	.006

Table 2. *Continued*

Region[a]	Hemisphere	Cluster Size[b]	Cluster Peak[c] (mm, MNI)			CBVa (ml Blood/100 ml Tissue)				Relative Change (%)[d]	Effect Size[e]	Adjusted *P* Value
						Schizophrenia		Control				
			x	y	z	Mean	SD	Mean	SD			
Postcentral	L	554	−44	−42	64	0.77	0.24	1.18	0.37	−34.9	−1.36	.017
Postcentral	R	363	64	−16	14	0.84	0.19	1.20	0.38	−30.3	−1.26	.026
Precentral	L	479	−52	6	34	0.86	0.20	1.21	0.32	−28.9	−1.38	.016
Precentral	R	201	12	−32	74	0.85	0.23	1.46	0.91	−41.9	−0.96	.05
Precuneus	L	520	−2	−74	52	0.79	0.20	1.14	0.15	−30.6	−2.05	.002
Precuneus	R	506	4	−68	48	0.84	0.16	1.17	0.13	−28.6	−2.34	.001
Rolandic_Oper	L	97	−60	10	2	1.05	0.24	1.52	0.58	−31.0	−1.10	.048
Rolandic_Oper	R	166	60	−14	14	1.27	0.72	1.92	0.50	−33.8	−1.09	.03
Supp_Motor_Area	L	291	−2	4	52	0.89	0.26	1.55	0.52	−42.9	−1.68	.005
Supp_Motor_Area	R	441	6	12	66	0.94	0.25	1.50	0.41	−37.3	−1.73	.004
SupraMarginal	L	231	−64	−44	34	0.88	0.20	1.19	0.25	−26.0	−1.41	.013
SupraMarginal	R	153	64	−18	22	0.98	0.11	1.23	0.25	−20.3	−1.34	.019
Temporal_Mid	L	1041	−52	−52	12	1.16	0.14	1.92	0.94	−39.3	−1.16	.016
Temporal_Mid	R	450	60	−50	−2	1.17	0.30	1.96	0.93	−40.5	−1.19	.05
Temporal_Sup	L	523	−50	−8	−6	1.17	0.25	1.86	0.57	−36.8	−1.62	.007
Temporal_Sup	R	791	60	−12	−8	1.15	0.55	1.99	0.92	−42.2	−1.15	.016
Thalamus	L	37	−6	−6	0	0.91	0.17	1.11	0.12	−18.0	−1.42	.015
Thalamus	R	47	10	−26	6	0.88	0.15	1.03	0.04	−14.4	−1.39	.028

Note: GM, grey matter; MNI, Montreal Neurological Institute.
[a]The brain regions were labeled according to the IBASPM 116 atlas (please see Methods for references).
[b]Number of voxels that show significant group difference in this region.
[c]Location of the voxel with the maximum (peak) T-score in the cluster in the MNI space.
[d]Relative change was defined as 100 × (mean CBVa in schizophrenia − mean CBVa in controls) / (mean CBVa in controls) %.
[e]Effect size was estimated with Cohen's d = (mean CBVa in schizophrenia − mean CBVa in controls)/ s, where s is the pooled SD of the 2 groups.

Table 3. Increased GM CBVa in Schizophrenia Patients Compared to Controls in Various Brain Regions

Region[a]	Hemisphere	Cluster Size[b]	Cluster Peak[c] (mm, MNI)			CBVa (ml Blood/100 ml Tissue)				Relative Change (%)[d]	Effect Size[e]	Adjusted *P* Value
						Schizophrenia		Control				
			x	y	z	Mean	SD	Mean	SD			
Angular	R	18	54	−52	36	1.18	0.21	0.93	0.22	27.4	1.24	.026
Calcarine	L	93	−4	−94	−12	1.02	0.03	0.76	0.35	33.7	1.06	.05
Cerebelum_4_5	R	24	14	−46	−14	1.70	1.38	1.07	0.50	59.1	0.63	.05
Cingulum_Mid	R	41	6	18	42	1.18	0.23	1.01	0.06	16.6	1.02	.05
Frontal_Inf_Oper	R	55	62	14	26	1.64	0.73	1.09	0.16	50.7	1.08	.05
Frontal_Mid	R	55	24	54	26	1.64	0.85	1.03	0.25	59.2	1.01	.05
Fusiform	L	35	−32	−52	−6	1.10	0.26	0.86	0.28	26.9	0.88	.05
Hippocampus	L	12	−34	−34	−6	1.04	0.11	0.88	0.23	18.2	0.93	.05
Hippocampus	R	18	38	−34	−10	1.90	1.33	1.02	0.35	85.6	0.94	.05
Lingual	L	54	−18	−60	−6	1.04	0.11	0.89	0.23	17.8	0.93	.05
Lingual	R	99	10	−84	−10	1.12	0.17	0.89	0.23	26.1	1.18	.033
Occipital_Inf	L	63	−16	−96	−10	1.05	0.11	0.77	0.42	35.4	0.93	.05
Occipital_Inf	R	22	36	−68	−8	1.09	0.18	0.84	0.32	29.5	0.99	.05
Occipital_Mid	R	28	46	−78	32	1.12	0.22	0.88	0.19	27.0	1.21	.031
Parietal_Inf	R	33	54	−48	40	1.22	0.20	0.99	0.08	23.4	1.59	.013
Postcentral	R	66	60	−2	32	1.20	0.22	1.02	0.08	17.8	1.14	.05
Precentral	R	87	50	10	36	1.17	0.19	0.99	0.05	18.6	1.37	.03
SupraMarginal	R	71	64	−44	36	1.20	0.21	1.01	0.03	18.5	1.31	.038

Note: [a]The brain regions were labeled according to the IBASPM 116 atlas (please see Methods for references).
[b]Number of voxels that show significant group difference in this region.
[c]Location of the voxel with the maximum (peak) T-score in the cluster in the MNI space.
[d]Relative change was defined as 100 × (mean CBVa in schizophrenia − mean CBVa in controls) / (mean CBVa in controls) %.
[e]Effect size was estimated with Cohen's d = (mean CBVa in schizophrenia − mean CBVa in controls)/ s, where s is the pooled SD of the 2 groups.

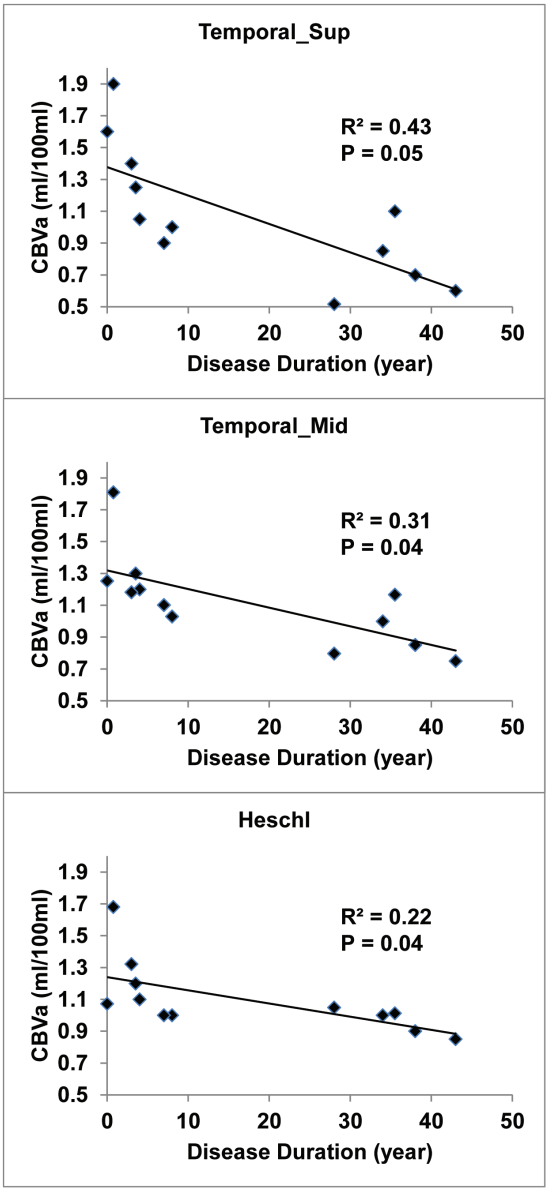

Fig. 2. Correlations analysis. Scatter plots showing correlations between grey matter (GM) arteriolar cerebral blood volume (CBVa) in the superior temporal gyrus ("Temporal_Sup"), middle temporal gyrus ("Temporal_Mid"), and Heschl gyrus ("Heschl," also known as transverse temporal gyrus), and disease duration in schizophrenia patients. R^2: adjusted R^2 from linear regression. Age, smoking status and medication dosage were included as covariates in the correlation analysis.

precuneus,[28,31] cingulate cortex,[22,25,26] fusiform,[22] insula,[25] and thalamus.[32,35] In addition to these areas, we identified additional regions with decreased GM CBVa, including the angular gyrus, cuneus, Heschl's gyrus, lingual gyrus and the sensorimotor regions, all of which have been implicated in schizophrenia.[74] Interestingly, a similar study from our group using iVASO MRI at 7T found *increased rather than decreased* GM CBVa in many of the same brain regions in Huntington's disease,[55] demonstrating specificity of our current findings and suggesting that the CBVa abnormalities detected in schizophrenia are not likely due to some undetected systemic bias or artifact.

The GM CBVa values in schizophrenia patients showed significant correlations with disease duration in several regions in the temporal cortex, such as the superior and middle temporal gyri and the Heschl's gyrus. The temporal lobe is thought to be one of the most relevant brain regions to schizophrenia,[75,76] with evidence of volume reduction[77–80] and deficits in activity during functional tasks as measured by event-related potential (ERP),[81] PET,[82] and fMRI,[83,84] and abnormal functional connectivity.[85–87] Heschl's gyrus, also known as the transverse temporal gyrus, forms part of the primary auditory cortex, and is the first functional unit processing incoming auditory information. Given the salience of auditory hallucinations to schizophrenia, deficits in the auditory cortex of individuals with schizophrenia have received considerable attention.[83,88,89] The significant correlations between CBVa and disease duration that we detected in these regions of the temporal cortex suggest that CBVa could be a sensitive and quantitative indicator for tracking disease progression in schizophrenia. No correlation between CBVa and clinical symptoms (BPRS and subscales) and cognitive functions (MoCA and subscales) reached statistical significance in our data, possibly due to limited sample size. Future studies are merited to investigate the link between regional CBVa levels and symptoms of psychosis such as delusion[10] in order to validate CBVa as a potential biomarker for schizophrenia.

Several brain regions with significantly increased GM CBVa were also identified in our data, although the number and size of the regions were much smaller than those with decreased CBVa. Further investigation with a larger sample size is warranted to validate these effects. Increased total CBV and/or CBF in schizophrenia have previously been described in regions including the cerebellum,[18,19,22,26,29] occipital cortex,[19] frontal cortex,[10,35,90] cingulate cortex,[29] and hippocampus.[5,10,20–22,28] Our data indicate both decreased and increased GM CBVa values in some of these regions, which implies that different subregions in one brain structure can be affected differently by the neuropathology of schizophrenia. Indeed, similar heterogeneity was demonstrated in a recent study that found increased total CBV in the CA1 subfield of the hippocampus, but a trend of decreased total CBV in CA2 and CA3 subfields in schizophrenia patients.[20] This type of regional heterogeneity might be one of the factors that contribute to some of the inconsistent results reported in previous studies on brain perfusion in schizophrenia.

A prominent line of argument is that the pathophysiology of schizophrenia is restricted to particular regions of the brain, such as the prefrontal cortex.[91,92] Many imaging studies have also emphasized these selective regions.[16,17,30] On the other hand, evidence has emerged of much more widespread abnormalities.[25,31,93] Our data, demonstrating changes in CBVa in multiple cortical and sub-cortical

regions, is consistent with this latter hypothesis, with implications for the type of pathophysiology underlying schizophrenia.

A vascular theory for the pathogenesis of schizophrenia has been proposed,[6] which postulates that the impaired microvascular system disrupts the regulation of energy supply for brain tissues and eventually leads to metabolic abnormalities in the brain and the schizophrenia clinical syndrome. Although no such causal relationship can be inferred from our present study, our results provide some evidence that microvasculature anomalies may be an important component in the pathogenesis of schizophrenia. Such abnormalities in the cerebral vasculature have also been detected at the molecular and cellular levels in postmortem brain tissue studies. Transcriptional alterations in the cerebral vascular endothelial cells isolated from brain tissues from schizophrenia patients have been demonstrated using laser capture microdissection.[94] An electron microscopy study revealed that the number of pericapillary oligodendrocytes in the prefrontal cortex was significantly lower in schizophrenia patients compared to controls.[95] Astrocytes are important glial cells that can regulate the contractility of some of the intracerebral arteries.[96–98] A recent study demonstrated that the volume fraction and area density of the mitochondria in the astrocytes from the brains of schizophrenia patients correlated negatively with disease duration.[99] Immunohistological studies have also suggested decreased numbers of astrocytes adjacent to blood vessels in the prefrontal and cingulate cortex and the hippocampus in schizophrenia.[100,101] These molecular and cellular deficits reported in schizophrenia all support our observation of altered cerebral vasculature in the current study. Further investigation is required to determine whether the vascular abnormalities observed here reflect a fundamental pathogenic process in schizophrenia, a secondary but contributing factor in the pathogenesis, or an epiphenomenon. Regardless of the pathogenic relevance, the microvascular changes detected here may have potential to be used as a quantitative marker for the disease.

Our results must be interpreted in the light of several potential confounding effects. First, regional atrophy in the brain has been documented in schizophrenia,[18,30,32,37,80,102] which may distort GM CBVa values in patients due to partial volume effects, the distinct CBVa values in WM, and the absence of CBV in CSF. To correct for this confounding factor, we adopted a previously published correction method[64] when calculating the iVASO difference signals in GM (see Methods section). We also included GM volume derived from high resolution anatomical images as a covariate in all subsequent statistical analyses to account for any residual partial volume effects. Importantly, as noted above, in a study of Huntington's disease using the same methodology,[55] we found increased (instead of decreased) GM CBVa in patients who have more prominent regional brain atrophy than schizophrenia patients in this study. Secondly, it is well-known that tobacco use is more prevalent in schizophrenia patients than the general population, and that chronic smoking significantly alters cerebral perfusion.[103] Therefore, the current smoking status of each study participant was recorded in cigarettes smoked per day, and the average numbers were comparable between controls and patients in this study. Moreover, smoking status was included as a covariate for group comparison and correlation analysis here. A more detailed investigation on the effects from smoking on CBVa is merited, and a quantity better reflecting the cumulative tobacco exposure of the participants such as pack-year should be used in such follow-up studies. Thirdly, the GM CBVa values in a few sub-regions in controls (tables 2 and 3) showed some discrepancies compared to values reported in our previous studies of normal subjects (1.27 ± 0.13 ml/100 ml averaged in *cortical* GM).[48] While tobacco use in controls may potentially contribute to this discrepancy, some brain regions may be more sensitive to large-vessel partial voluming and CSF pulsation effects in iVASO MRI.[48] Nevertheless, as these technical effects are likely to affect data from patients and controls in a similar manner, we expect negligible influence on our main findings from group comparisons. Finally, an important caveat is that the patients, not controls, in this study were all receiving antipsychotic medicines. Whether such antipsychotic drugs themselves affect cerebral perfusion, or the extent to which the therapeutic effect of antipsychotics normalizes cerebral perfusion, remains to be determined. Previous studies that attempted to address this question are inconsistent, with some evidence that antipsychotics have no effect on total CBV[5,10,14,20] and CBF,[95,104,105] but contrary evidence has also been reported.[106–110] A further complication is that different pharmacological classes of antipsychotics may have a different effect on cerebral perfusion.[111] In our data, no significant correlation was found between CBVa and medication dosage in patients; and medication dosage was included as a covariate when assessing correlations between CBVa and disease duration, BPRS and MOCA scores (including subscales). Future study is merited to determine if CBVa abnormalities are also presenting in unmedicated patients, and to determine whether antipsychotics differentially affect different brain regions.

Conclusion

We report widespread reduction in CBVa in the GM of schizophrenia patients. GM CBVa values in several regions in the temporal cortex correlated negatively with disease duration in patients. Increase in GM CBVa was also found in a few cortical and sub-cortical regions. Our results indicate that microvascular abnormalities may be a fundamental aspect of the pathogenesis of schizophrenia, and that brain changes in schizophrenia appear to

be widespread. Future studies with a larger cohort and longitudinal follow-up are merited to determine the onset and characterize the progression of GM CBVa changes, and to determine whether CBVa could be used as a potential marker for brain changes in schizophrenia.

Supplementary Material

Supplementary material is available at http://schizophreniabulletin.oxfordjournals.org.

Funding

This project was supported by a generous donation from Mr Jose Brito, and by the National Center for Research Resources and the National Institute of Biomedical Imaging and Bioengineering of the National Institutes of Health through resource grant P41 EB015909, and by the National Institute of Mental Health of the National Institutes of Health through grant R21 MH107016. J.H.'s salary was paid in part from a grant to the Kennedy Krieger Institute from Philips Healthcare. Equipment used in the study was manufactured by Philips. P.C.M.v.Z. is a paid lecturer for Philips Healthcare. This arrangement has been approved by Johns Hopkins University in accordance with its conflict of interest policies.

Acknowledgments

The authors thank Mr Joseph S. Gillen, Mrs Terri Lee Brawner, Ms Kathleen A. Kahl, and Ms Ivana Kusevic for experimental assistance. The authors have declared that there are no conflicts of interest in relation to the subject of this study.

References

1. Mueser KT, McGurk SR. Schizophrenia. *Lancet*. 2004;363:2063–2072.
2. Harvey PD, Reichenberg A, Bowie CR, Patterson TL, Heaton RK. The course of neuropsychological performance and functional capacity in older patients with schizophrenia: influences of previous history of long-term institutional stay. *Biol Psychiatry*. 2010;67:933–939.
3. Manji H, Kato T, Di Prospero NA, et al. Impaired mitochondrial function in psychiatric disorders. *Nat Rev Neurosci*. 2012;13:293–307.
4. Martins-de-Souza D, Harris LW, Guest PC, Bahn S. The role of energy metabolism dysfunction and oxidative stress in schizophrenia revealed by proteomics. *Antioxid Redox Signal*. 2011;15:2067–2079.
5. Schobel SA, Chaudhury NH, Khan UA, et al. Imaging patients with psychosis and a mouse model establishes a spreading pattern of hippocampal dysfunction and implicates glutamate as a driver. *Neuron*. 2013;78:81–93.
6. Hanson DR, Gottesman II. Theories of schizophrenia: a genetic-inflammatory-vascular synthesis. *BMC Med Genet*. 2005;6:7.
7. Raz L, Knoefel J, Bhaskar K. The neuropathology and cerebrovascular mechanisms of dementia. *J Cereb Blood Flow Metab*. 2016;36:172–186.
8. Gonzalez RG, Fischman AJ, Guimaraes AR, et al. Functional MR in the evaluation of dementia: correlation of abnormal dynamic cerebral blood volume measurements with changes in cerebral metabolism on positron emission tomography with fludeoxyglucose F 18. *AJNR Am J Neuroradiol*. 1995;16:1763–1770.
9. Raichle ME. Positron emission tomography. *Annu Rev Neurosci*. 1983;6:249–267.
10. Schobel SA, Lewandowski NM, Corcoran CM, et al. Differential targeting of the CA1 subfield of the hippocampal formation by schizophrenia and related psychotic disorders. *Arch Gen Psychiatry*. 2009;66:938–946.
11. van Zijl PC, Eleff SM, Ulatowski JA, et al. Quantitative assessment of blood flow, blood volume and blood oxygenation effects in functional magnetic resonance imaging. *Nat Med*. 1998;4:159.
12. Ogawa S, Menon RS, Tank DW, et al. Functional brain mapping by blood oxygenation level-dependent contrast magnetic resonance imaging. A comparison of signal characteristics with a biophysical model. *Biophys J*. 1993;64:803.
13. Buxton RB, Frank LR. A model for the coupling between cerebral blood flow and oxygen metabolism during neural stimulation. *J Cereb Blood Flow Metab*. 1997;17:64–72.
14. Brambilla P, Cerini R, Fabene PF, et al. Assessment of cerebral blood volume in schizophrenia: a magnetic resonance imaging study. *J Psychiatr Res*. 2007;41:502–510.
15. Uh J, Mihalakos P, Tamminga CA, Lu H. Perfusion deficit in schizophrenia and correlation with psychopathological symptoms. Paper presented at: Proc. 17th Annual Meeting ISMRM; April 2009; Hawaii, HI.
16. Peruzzo D, Rambaldelli G, Bertoldo A, et al. The impact of schizophrenia on frontal perfusion parameters: a DSC-MRI study. *J Neural Transm*. 2011;118:563–570.
17. Bellani M, Peruzzo D, Isola M, et al. Cerebellar and lobar blood flow in schizophrenia: a perfusion weighted imaging study. *Psychiatry Res*. 2011;193:46–52.
18. Loeber RT, Sherwood AR, Renshaw PF, Cohen BM, Yurgelun-Todd DA. Differences in cerebellar blood volume in schizophrenia and bipolar disorder. *Schizophr Res*. 1999;37:81–89.
19. Cohen BM, Yurgelun-Todd D, English CD, Renshaw PF. Abnormalities of regional distribution of cerebral vasculature in schizophrenia detected by dynamic susceptibility contrast MRI. *Am J Psychiatry*. 1995;152:1801–1803.
20. Talati P, Rane S, Kose S, et al. Increased hippocampal CA1 cerebral blood volume in schizophrenia. *NeuroImage Clinical* 2014;5:359–364.
21. Tamminga CA, Southcott S, Sacco C, Wagner AD, Ghose S. Glutamate dysfunction in hippocampus: relevance of dentate gyrus and CA3 signaling. *Schizophr Bull*. 2012;38:927–935.
22. Malaspina D, Harkavy-Friedman J, Corcoran C, et al. Resting neural activity distinguishes subgroups of schizophrenia patients. *Biol Psychiatry*. 2004;56:931–937.
23. Schultz SK, O'Leary DS, Boles Ponto LL, et al. Age and regional cerebral blood flow in schizophrenia: age effects in anterior cingulate, frontal, and parietal cortex. *J Neuropsychiatry Clin Neurosci*. 2002;14:19–24.
24. Weinberger DR, Berman KF, Zec RF. Physiologic dysfunction of dorsolateral prefrontal cortex in schizophrenia.

I. Regional cerebral blood flow evidence. *Arch Gen Psychiatry*. 1986;43:114–124.
25. Zhu J, Zhuo C, Qin W, et al. Altered resting-state cerebral blood flow and its connectivity in schizophrenia. *J Psychiatr Res*. 2015;63:28–35.
26. Scheef L, Manka C, Daamen M, et al. Resting-state perfusion in nonmedicated schizophrenic patients: a continuous arterial spin-labeling 3.0-T MR study. *Radiology*. 2010;256:253–260.
27. Faget-Agius C, Boyer L, Padovani R, et al. Schizophrenia with preserved insight is associated with increased perfusion of the precuneus. *J Psychiatry Neurosci*. 2012;37:297–304.
28. Eisenberg DP, Sarpal D, Kohn PD, et al. Catechol-o-methyltransferase valine(158)methionine genotype and resting regional cerebral blood flow in medication-free patients with schizophrenia. *Biol Psychiatry*. 2010;67:287–290.
29. Andreasen NC, O'Leary DS, Flaum M, et al. Hypofrontality in schizophrenia: distributed dysfunctional circuits in neuroleptic-naive patients. *Lancet*. 1997;349:1730–1734.
30. Ota M, Ishikawa M, Sato N, et al. Pseudo-continuous arterial spin labeling MRI study of schizophrenic patients. *Schizophr Res*. 2014;154:113–118.
31. Pinkham A, Loughead J, Ruparel K, et al. Resting quantitative cerebral blood flow in schizophrenia measured by pulsed arterial spin labeling perfusion MRI. *Psychiatry Res*. 2011;194:64–72.
32. Walther S, Federspiel A, Horn H, et al. Resting state cerebral blood flow and objective motor activity reveal basal ganglia dysfunction in schizophrenia. *Psychiatry Res*. 2011;192:117–124.
33. Kanahara N, Sekine Y, Haraguchi T, et al. Orbitofrontal cortex abnormality and deficit schizophrenia. *Schizophr Res*. 2013;143:246–252.
34. Kindler J, Jann K, Homan P, et al. Static and dynamic characteristics of cerebral blood flow during the resting state in schizophrenia. *Schizophr Bull*. 2015;41:163–170.
35. Tsujino N, Nemoto T, Yamaguchi T, et al. Cerebral blood flow changes in very-late-onset schizophrenia-like psychosis with catatonia before and after successful treatment. *Psychiatry Clin Neurosci*. 2011;65:600–603.
36. Uranova NA, Zimina IS, Vikhreva OV, Krukov NO, Rachmanova VI, Orlovskaya DD. Ultrastructural damage of capillaries in the neocortex in schizophrenia. *World J Biol Psychiatry*. 2010;11:567–578.
37. Kreczmanski P, Schmidt-Kastner R, Heinsen H, Steinbusch HW, Hof PR, Schmitz C. Stereological studies of capillary length density in the frontal cortex of schizophrenics. *Acta Neuropathol*. 2005;109:510–518.
38. Kreczmanski P, Heinsen H, Mantua V, et al. Microvessel length density, total length, and length per neuron in five subcortical regions in schizophrenia. *Acta Neuropathol*. 2009;117:409–421.
39. Attwell D, Buchan AM, Charpak S, Lauritzen M, Macvicar BA, Newman EA. Glial and neuronal control of brain blood flow. *Nature*. 2010;468:232–243.
40. Attwell D, Iadecola C. The neural basis of functional brain imaging signals. *Trends Neurosci*. 2002;25:621.
41. Iadecola C, Nedergaard M. Glial regulation of the cerebral microvasculature. *Nat Neurosci*. 2007;10:1369–1376.
42. Ito H, Ibaraki M, Kanno I, Fukuda H, Miura S. Changes in the arterial fraction of human cerebral blood volume during hypercapnia and hypocapnia measured by positron emission tomography. *J Cereb Blood Flow Metab*. 2005;25:852–857.
43. Ito H, Kanno I, Iida H, et al. Arterial fraction of cerebral blood volume in humans measured by positron emission tomography. *Ann Nucl Med*. 2001;15:111.
44. Kim T, Hendrich KS, Masamoto K, Kim SG. Arterial versus total blood volume changes during neural activity-induced cerebral blood flow change: implication for BOLD fMRI. *J Cereb Blood Flow Metab*. 2007;27:1235–1247.
45. Takano T, Tian GF, Peng W, et al. Astrocyte-mediated control of cerebral blood flow. *Nat Neurosci*. 2006;9:260.
46. Koehler RC, Roman RJ, Harder DR. Astrocytes and the regulation of cerebral blood flow. *Trends Neurosci*. 2009;32:160–169.
47. Winkler EA, Bell RD, Zlokovic BV. Central nervous system pericytes in health and disease. *Nat Neurosci*. 2011;14:1398–1405.
48. Hua J, Qin Q, Pekar JJ, Zijl PC. Measurement of absolute arterial cerebral blood volume in human brain without using a contrast agent. *NMR Biomed*. 2011;24:1313–1325.
49. Hua J, Qin Q, Donahue MJ, Zhou J, Pekar JJ, van Zijl PC. Inflow-based vascular-space-occupancy (iVASO) MRI. *Magn Reson Med*. 2011;66:40–56.
50. Donahue MJ, Sideso E, MacIntosh BJ, Kennedy J, Handa A, Jezzard P. Absolute arterial cerebral blood volume quantification using inflow vascular-space-occupancy with dynamic subtraction magnetic resonance imaging. *J Cereb Blood Flow Metab*. 2010;30:1329–1342.
51. Donahue MJ, MacIntosh BJ, Sideso E, et al. Absolute cerebral blood volume (CBV) quantification without contrast agents using inflow vascular-space-occupancy (iVASO) with dynamic subtraction. Paper presented at: Proc. 17th Annual Meeting ISMRM; April 2009; Hawaii, HI.
52. Hua J, Qin Q, Donahue MJ, Zhou J, Pekar J, van Zijl PCM. Functional MRI Using Arteriolar Cerebral Blood Volume Changes. Paper presented at: Proc. 17th Annual Meeting ISMRM; April 2009; Hawaii, HI.
53. Hua J, Qin Q, Pekar J, van Zijl PCM. Measuring Absolute Arteriolar Cerebral Blood Volume (CBVa) in Human Brain Gray Matter (GM) without Contrast Agent. Paper presented at: Proc. 17th Annual Meeting ISMRM; April 2009; Hawaii, HI.
54. Rane S, Talati P, Donahue MJ, Heckers S. Inflow-vascular space occupancy (iVASO) reproducibility in the hippocampus and cortex at different blood water nulling times. *Magn Reson Med*. 2016;75:2379–2387.
55. Hua J, Unschuld PG, Margolis RL, van Zijl PC, Ross CA. Elevated arteriolar cerebral blood volume in prodromal Huntington's disease. *Mov Disord*. 2014;29:396–401.
56. Hua J, Lee S, Blair NIS, et al. Reduced grey matter arteriolar cerebral blood volume in schizophrenia. Paper presented at: Proc. 23rd Annual Meeting ISMRM; June 2015; Toronto, Ontario, Canada.
57. Overall JE, Gorham DR. The Brief Psychiatric Rating Scale. *Psychol Rep* 1962;10:799–812.
58. Nasreddine ZS, Phillips NA, Bedirian V, et al. The Montreal Cognitive Assessment, MoCA: a brief screening tool for mild cognitive impairment. *J Am Geriatr Soc*. 2005;53:695–699.
59. Marques JP, Kober T, Krueger G, van der Zwaag W, Van de Moortele PF, Gruetter R. MP2RAGE, a self bias-field corrected sequence for improved segmentation and T1-mapping at high field. *Neuroimage*. 2010;49:1271–1281.
60. Van de Moortele PF, Auerbach EJ, Olman C, Yacoub E, Ugurbil K, Moeller S. T1 weighted brain images at 7 Tesla unbiased for Proton Density, T2* contrast and RF coil

receive B1 sensitivity with simultaneous vessel visualization. *Neuroimage*. 2009;46:432–446.

61. Hua J, Jones CK, Qin Q, van Zijl PC. Implementation of vascular-space-occupancy MRI at 7T. *Magn Reson Med*. 2013;69:1003–1013.
62. Rooney WD, Johnson G, Li X, et al. Magnetic field and tissue dependencies of human brain longitudinal 1H2O relaxation in vivo. *Magn Reson Med*. 2007;57:308–318.
63. Lu H, Donahue MJ, van Zijl PC. Detrimental effects of BOLD signal in arterial spin labeling fMRI at high field strength. *Magn Reson Med*. 2006;56:546–552.
64. Johnson NA, Jahng GH, Weiner MW, et al. Pattern of cerebral hypoperfusion in Alzheimer disease and mild cognitive impairment measured with arterial spin-labeling MR imaging: initial experience. *Radiology*. 2005;234:851–859.
65. Maldjian JA, Laurienti PJ, Burdette JH. Precentral gyrus discrepancy in electronic versions of the Talairach atlas. *Neuroimage*. 2004;21:450–455.
66. Maldjian JA, Laurienti PJ, Kraft RA, Burdette JH. An automated method for neuroanatomic and cytoarchitectonic atlas-based interrogation of fMRI data sets. *Neuroimage*. 2003;19:1233–1239.
67. Lancaster JL, Woldorff MG, Parsons LM, et al. Automated Talairach atlas labels for functional brain mapping. *Hum Brain Mapp*. 2000;10:120–131.
68. Lancaster JL, Rainey LH, Summerlin JL, et al. Automated labeling of the human brain: a preliminary report on the development and evaluation of a forward-transform method. *Hum Brain Mapp*. 1997;5:238–242.
69. Tzourio-Mazoyer N, Landeau B, Papathanassiou D, et al. Automated anatomical labeling of activations in SPM using a macroscopic anatomical parcellation of the MNI MRI single-subject brain. *Neuroimage*. 2002;15:273–289.
70. Rosner B. *Fundamentals of Biostatistics*. 7th ed. Boston, MA: Brooks/Cole; 2011.
71. Grobner T. Gadolinium--a specific trigger for the development of nephrogenic fibrosing dermopathy and nephrogenic systemic fibrosis? *Nephrol Dial Transplant*. 2006;21:1104–1108.
72. Marckmann P, Skov L, Rossen K, et al. Nephrogenic systemic fibrosis: suspected causative role of gadodiamide used for contrast-enhanced magnetic resonance imaging. *J Am Soc Nephrol*. 2006;17:2359–2362.
73. McDonald RJ, McDonald JS, Kallmes DF, et al. Intracranial Gadolinium Deposition after Contrast-enhanced MR Imaging. *Radiology*. 2015;275:772–782.
74. Harrison PJ. The neuropathology of schizophrenia. a critical review of the data and their interpretation. *Brain*. 1999;122:593–624.
75. Pearlson GD. Superior temporal gyrus and planum temporale in schizophrenia: a selective review. *Prog Neuropsychopharmacol Biol Psychiatry*. 1997;21:1203–1229.
76. Pearlson GD, Petty RG, Ross CA, Tien AY. Schizophrenia: a disease of heteromodal association cortex? *Neuropsychopharmacology*. 1996;14:1–17.
77. Soares JC, Mann JJ. The anatomy of mood disorders–review of structural neuroimaging studies. *Biol Psychiatry*. 1997;41:86–106.
78. Strakowski SM, DelBello MP, Sax KW, et al. Brain magnetic resonance imaging of structural abnormalities in bipolar disorder. *Arch Gen Psychiatry*. 1999;56:254–260.
79. Strasser HC, Lilyestrom J, Ashby ER, et al. Hippocampal and ventricular volumes in psychotic and nonpsychotic bipolar patients compared with schizophrenia patients and community control subjects: a pilot study. *Biol Psychiatry*. 2005;57:633–639.
80. Pearlson GD, Barta PE, Powers RE, et al. Ziskind-Somerfeld Research Award 1996. Medial and superior temporal gyral volumes and cerebral asymmetry in schizophrenia versus bipolar disorder. *Biol Psychiatry*. 1997;41:1–14.
81. McCarley RW, Faux SF, Shenton ME, Nestor PG, Adams J. Event-related potentials in schizophrenia: their biological and clinical correlates and a new model of schizophrenic pathophysiology. *Schizophr Res*. 1991;4:209–231.
82. Fletcher PC, McKenna PJ, Frith CD, Grasby PM, Friston KJ, Dolan RJ. Brain activations in schizophrenia during a graded memory task studied with functional neuroimaging. *Arch Gen Psychiatry*. 1998;55:1001–1008.
83. Kiehl KA, Liddle PF. An event-related functional magnetic resonance imaging study of an auditory oddball task in schizophrenia. *Schizophr Res*. 2001;48:159–171.
84. Calhoun VD, Kiehl KA, Liddle PF, Pearlson GD. Aberrant localization of synchronous hemodynamic activity in auditory cortex reliably characterizes schizophrenia. *Biol Psychiatry*. 2004;55:842–849.
85. Calhoun VD, Maciejewski PK, Pearlson GD, Kiehl KA. Temporal lobe and "default" hemodynamic brain modes discriminate between schizophrenia and bipolar disorder. *Hum Brain Mapp*. 2008;29:1265–1275.
86. Fletcher P, McKenna PJ, Friston KJ, Frith CD, Dolan RJ. Abnormal cingulate modulation of fronto-temporal connectivity in schizophrenia. *Neuroimage*. 1999;9:337–342.
87. Çetin MS, Christensen F, Abbott CC, et al. Thalamus and posterior temporal lobe show greater inter-network connectivity at rest and across sensory paradigms in schizophrenia. *Neuroimage*. 2014;97:117–126.
88. Chun S, Westmoreland JJ, Bayazitov IT, et al. Specific disruption of thalamic inputs to the auditory cortex in schizophrenia models. *Science*. 2014;344:1178–1182.
89. Shi WX. The auditory cortex in schizophrenia. *Biol Psychiatry*. 2007;61:829–830.
90. Catafau AM, Parellada E, Lomena FJ, et al. Prefrontal and temporal blood flow in schizophrenia: resting and activation technetium-99m-HMPAO SPECT patterns in young neuroleptic-naive patients with acute disease. *J Nucl Med*. 1994;35:935–941.
91. Selemon LD, Zecevic N. Schizophrenia: a tale of two critical periods for prefrontal cortical development. *Transl Psychiatry*. 2015;5:e623.
92. Sakurai T, Gamo NJ, Hikida T, et al. Converging models of schizophrenia - Network alterations of prefrontal cortex underlying cognitive impairments. *Prog Neurobiol*. 2015;134:178–201.
93. Reading SA, Oishi K, Redgrave GW, et al. Diffuse abnormality of low to moderately organized white matter in schizophrenia. *Brain Connect*. 2011;1:511–519.
94. Harris LW, Wayland M, Lan M, et al. The cerebral microvasculature in schizophrenia: a laser capture microdissection study. *PLoS One*. 2008;3:e3964.
95. Vostrikov V, Orlovskaya D, Uranova N. Deficit of pericapillary oligodendrocytes in the prefrontal cortex in schizophrenia. *World J Biol Psychiatry*. 2008;9:34–42.
96. Zlokovic BV. Neurovascular pathways to neurodegeneration in Alzheimer's disease and other disorders. *Nat Rev Neurosci*. 2011;12:723–738.
97. Takano T, Han X, Deane R, Zlokovic B, Nedergaard M. Two-photon imaging of astrocytic Ca2+ signaling and the

microvasculature in experimental mice models of Alzheimer's disease. *Ann N Y Acad Sci*. 2007;1097:40–50.

98. Kuchibhotla KV, Lattarulo CR, Hyman BT, Bacskai BJ. Synchronous hyperactivity and intercellular calcium waves in astrocytes in Alzheimer mice. *Science*. 2009;323:1211–1215.
99. Kolomeets NS, Uranova N. Ultrastructural abnormalities of astrocytes in the hippocampus in schizophrenia and duration of illness: a postortem morphometric study. *World J Biol Psychiatry*. 2010;11:282–292.
100. Webster MJ, Knable MB, Johnston-Wilson N, Nagata K, Inagaki M, Yolken RH. Immunohistochemical localization of phosphorylated glial fibrillary acidic protein in the prefrontal cortex and hippocampus from patients with schizophrenia, bipolar disorder, and depression. *Brain Behav Immun*. 2001;15:388–400.
101. Webster MJ, O'Grady J, Kleinman JE, Weickert CS. Glial fibrillary acidic protein mRNA levels in the cingulate cortex of individuals with depression, bipolar disorder and schizophrenia. *Neuroscience*. 2005;133:453–461.
102. Meda SA, Giuliani NR, Calhoun VD, et al. A large scale (N=400) investigation of gray matter differences in schizophrenia using optimized voxel-based morphometry. *Schizophr Res*. 2008;101:95–105.
103. Gazdzinski S, Durazzo T, Jahng GH, Ezekiel F, Banys P, Meyerhoff D. Effects of chronic alcohol dependence and chronic cigarette smoking on cerebral perfusion: a preliminary magnetic resonance study. *Alcohol Clin Exp Res*. 2006;30:947–958.
104. Yildiz A, Eryilmaz M, Gungor F, Erkilic M, Karayalcin B. Regional cerebral blood flow in schizophrenia before and after neuroleptic medication. *Nucl Med Commun*. 2000;21:1113–1118.
105. Gonul AS, Kula M, Sofuoglu S, Tutus A, Esel E. Tc-99 HMPAO SPECT study of regional cerebral blood flow in olanzapine-treated schizophrenic patients. *Eur Arch Psychiatry Clin Neurosci*. 2003;253:29–33.
106. Handley R, Zelaya FO, Reinders AA, et al. Acute effects of single-dose aripiprazole and haloperidol on resting cerebral blood flow (rCBF) in the human brain. *Hum Brain Mapp*. 2013;34:272–282.
107. Matsuda H, Jibiki I, Kinuya K, et al. Tc-99m HMPAO SPECT analysis of neuroleptic effects on regional brain function. *Clin Nucl Med*. 1991;16:660–664.
108. Jibiki I, Matsuda H, Yamaguchi N, Kurokawa K, Hisada K. Acutely administered haloperidol-induced pattern changes of regional cerebral blood flow in schizophrenics. Observation from subtraction of brain imaging with single photon emission computed tomography using technetium-99m hexamethyl-propyleneamine oxime. *Neuropsychobiology*. 1992;25:182–187.
109. Miller DD, Rezai K, Alliger R, Andreasen NC. The effect of antipsychotic medication on relative cerebral blood perfusion in schizophrenia: assessment with technetium-99m hexamethyl-propyleneamine oxime single photon emission computed tomography. *Biol Psychiatry*. 1997;41:550–559.
110. Molina Rodríguez V, Montz Andreé R, Pérez Castejón MJ, Capdevila García E, Carreras Delgado JL, Rubia Vila FJ. SPECT study of regional cerebral perfusion in neuroleptic-resistant schizophrenic patients who responded or did not respond to clozapine. *Am J Psychiatry*. 1996;153:1343–1346.
111. Goozée R, Handley R, Kempton MJ, Dazzan P. A systematic review and meta-analysis of the effects of antipsychotic medications on regional cerebral blood flow (rCBF) in schizophrenia: association with response to treatment. *Neurosci Biobehav Rev*. 2014;43:118–136.